Available online at www.sciencedirect.com
ScienceDirect
Journal of Colloid and Interface Science 309 (2007) 373–383
JOURNAL OF Colloid and Interface Science
www.elsevier.com/locate/jcis

# Study of galactomannose interaction with solids using AFM, IR and allied techniques

Jing Wang, Ponisseril Somasundaran *

*NSF Industrial/University Cooperative Research Center for Advanced Studies in Novel Surfactants, Columbia University, New York, NY 10027, USA*

Received 6 October 2005; accepted 23 October 2006

Available online 9 November 2006

**Abstract**

Guar gum (GG) and locust bean gum (LBG) are two galactomannose polysaccharides with different mannose/galactose ratio which is widely used in many industrial sectors including food, textiles, paper, adhesive, paint, pharmaceuticals, cosmetics and mineral processing. They are natural nonionic polymers that are non-toxic and biodegradable. These properties make them ideal for industrial applications. However, a general lack of understanding of the interactions between the polysaccharides and solid surfaces has hindered wider application of these polymers. In this work, adsorption of locust bean gum and guar gum at the solid–liquid interface was investigated using adsorption tests, electrophoretic mobility measurements, FTIR, fluorescence spectroscopy, AFM and molecular modeling. Electrokinetic studies showed that the adsorption of GG and LBG on talc do not change its isoelectric point. In addition, GG and LBG adsorption on talc was found not to be affected by changes in solution conditions such as pH and ionic strength, which suggests a minor role of electrostatic force in adsorption. On the other hand, fluorescence spectroscopy studies conducted to investigate the role of hydrophobic bonding using pyrene probe showed no evidence of the formation of hydrophobic domains at talc–aqueous interface. Moreover, urea, a hydrogen bond breaker, markedly reduced the adsorption of LBG and GG on talc, supporting hydrogen bonding as an important role. In FTIR study, the changes in the infrared bands, associated with the C–O stretch coupled to the C–C stretch and O–H deformation, were significant and therefore also supporting hydrogen bonding of GG and LBG to the solid surface. In addition, Langmuir modeling of adsorption isotherm further suggested that hydrogen bonding is the dominant force for polysaccharide adsorption since the adsorption free energy of these polymers is close to that for hydrogen bond formation. From molecular modeling, different helical structures are observed for LBG and GG because of their different galactose/mannose ratio and these polymers were found to adsorb flat on solid to let more of its OH groups in contact with the surface. All of the above results suggest that the main driving force for adsorption both of GG and LBG on talc is hydrogen bonding rather than hydrophobic force even though there is difference in G/M ratio between them.


*Keywords:* Talc; Polysaccharide; Polymer adsorption; AFM; Model; Zeta potential; FTIR

## 1. Introduction

Talc is a layered hydrous magnesium silicate that consists of two different surfaces. Basal hydrophobic planes are formed by rupture of van der Waals bonds. However, the edges of the mineral sheets contain broken Si–O and Mg–O bonds and, consequently, are charged species and the edges exhibit hydrophilic properties.

Guar gum and locust bean gum are two natural nonionic polysaccharides with different ratio of galactose and mannose units. Galactomannans are the most common plant food reserve polysaccharides belonging to the legume family consisting of $\alpha$-(1-4)-linked D-mannan backbone grafted with $\alpha$-(1-6)-linked D-galactose stubs to some of the mannose residues [1] (see Fig. 1). Compared to GG, LBG and other galactomannans have been much less realized and applied in industrial fields. Therefore, it is essential to study the effect of galactose/mannose (G/M) ratio for exploring the structure–property relationship of different galactomanns. In this work, GG and LBG with G/M ratio of 1:2 and 1:3.5, respectively, were chosen to be studied. The OH groups on the repeating units are available for hydrogen bonding of the polymer molecule to mineral surfaces [2].

* Corresponding author.
*E-mail address:* ps24@columbia.edu (P. Somasundaran).

0021-9797/$ – see front matter 
doi:10.1016/j.jcis.2006.10.086

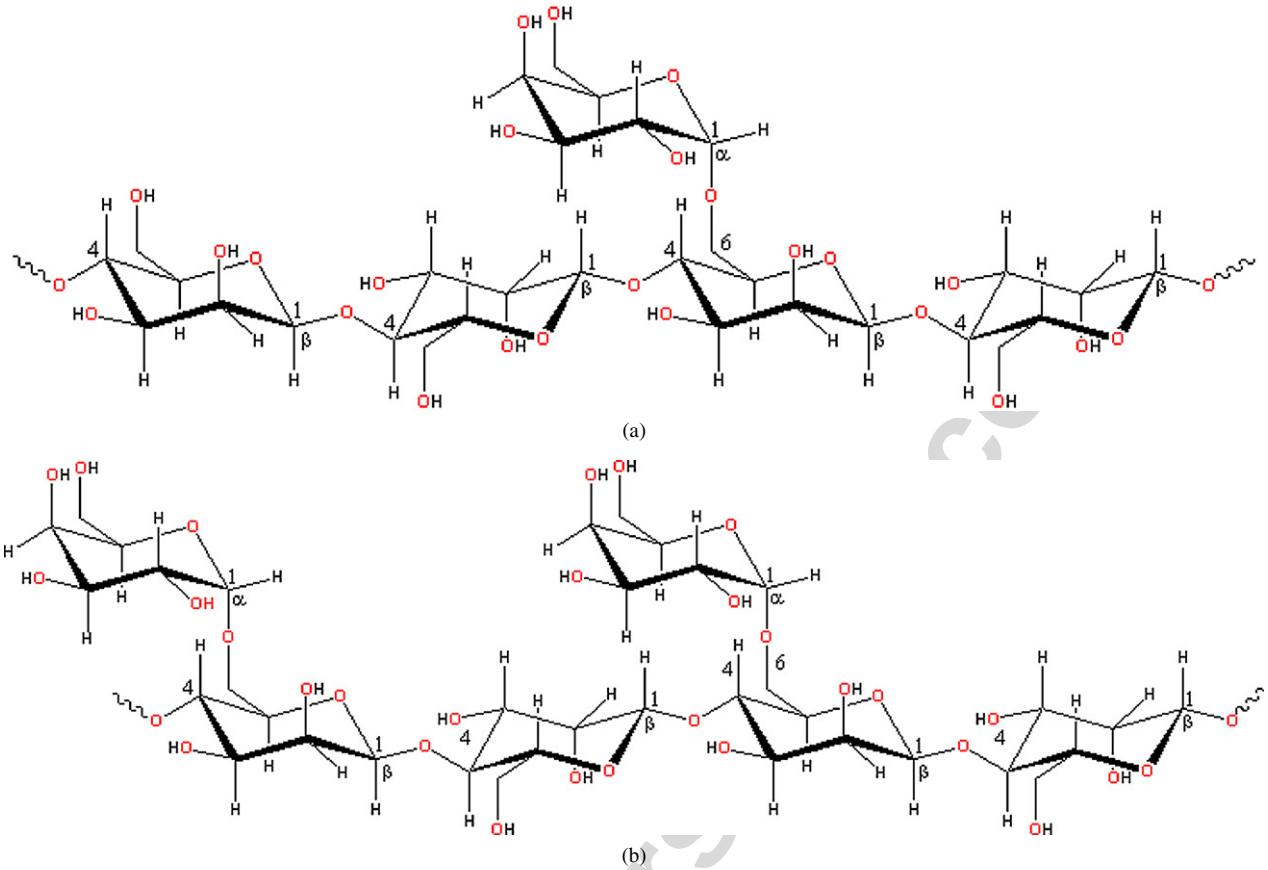

Fig. 1. The repeating unit structure of (a) locust bean gum and (b) guar gum.

The surface and interfacial properties of LBG and GG have been studied in some previous work [3–7]. Emulsification capabilities and stability of oil-in-water emulsions and adsorption isotherms have been determined and examined. In addition, LBG and GG were also investigated for their gelation and drug delivery properties [8,9]. In the mineral processing industry, guar gum is often used as a depressant for minerals. However, the interaction mechanism between these polymers and solids is not well understood. Mackenzie [10], Pugh [11], Healy [12] and Rath et al. [13,14] proposed that the mechanisms governing the adsorption of polymers on mineral surfaces include hydrophobic interaction, hydrogen bonding, chemical and electrostatic interactions. Steenberg et al. [15,16], Jenkins and Ralston [17] have proposed that the adsorption of guar gum on talc occurs mainly at the basal planes via hydrophobic force. In contrast, Rath et al. [18] and Jucker et al. [19] proposed that the adsorption of guar gum occurs through hydrogen bonding on solids. However the reasons for the selectivity of the adsorption of depressants on minerals has not been accounted for. In addition, almost no work has been done for exploring LBG–solid interaction.

The objective of this study was to clarify the mechanistic aspects of the interactions between these two nonionic polysaccharides and talc using a combination of adsorption, spectroscopic, microscopic, electrostatic and molecular modeling techniques.

## 2. Experimental

### 2.1. Materials

Talc sample of 40 μm size and BET surface area of 19.75 $m^2/g$ used for the present tests was obtained from Cytec Industries. The composition analysis was done by Galbraith Laboratory Inc. involved burning of the samples in a Schoniger flask and then reading the elemental composition using ionic electrode. The result indicates that it was a pure sample with only 0.7% tremolite ($Ca_2Mg_5Si_8O_{22}(OH)_2$). Mica in the form of flat plate purchased from Ted Pella Inc. was used in AFM studies.

The weight average molecular weight of guar gum obtained from Cytec Industries is 1,450,000. Locust bean gum of Mw of 1,000,000 was supplied by AEP colloids. All polymer stock solutions were prepared by quickly adding 0.045 g of gum powder into 45 ml of vigorously stirred water and further stirring for 30 min. The solution was refrigerated overnight to ensure complete hydration or dissolution of the polymer and then filtered through filter paper (Whatman #4) to remove any undissolved impurities.

pH of the solutions and suspensions was adjusted by Fisher standard hydrochloric acid or sodium hydroxide solutions. Reagent grade potassium chloride from APACHE Chemicals Inc. was used to adjust the ionic strength of solutions. 1-Pyrene butyric acid and 1,3-dicyclohexyl carbodiimide (DCC) bought

from Aldrich were used in the fluorescence probe labeling of polymers. Urea (Fisher Chemical), phenol (EM Science) and 98% sulfuric acid (Amend Drug & Chemical Co. Inc.) were used for colorimetric experiments. The water used was triply distilled.

### 2.2. Experiments

Experiments done along with the adsorption measurements to investigate the adsorption mechanisms involved include FTIR for exploring the role of hydrogen bonding in adsorption, fluorescence spectroscopy to study the role of hydrophobic forces, AFM and molecular modeling to explore the conformation of the adsorbed polysaccharides.

#### 2.2.1. Molecular modeling

Molecular modeling (Macromodel) was used to study the conformation of polysaccharides. Accelrys Material Studio was also used to estimate the conformation of adsorbed polysaccharides on solid surfaces.

#### 2.2.2. Electrokinetic measurements

Small amounts of talc was added to desired amounts of $10^{-3}$ M $KNO_3$ solution and ultrasonicated for 30 min, magnetically stirred for 2 h and the pH adjusted using HCl or KOH. Finally, the polymer stock solution was added and left for conditioning for 16 h. The zeta potential was then measured using a Zeta meter.

#### 2.2.3. Adsorption measurements

The 10% suspensions of solids, with pH and ionic strength adjusted to the desired level using KCl, HCl or KOH, were ultrasonicated for 30 min and then stirred magnetically for 2 h. Polymer stock solution was then added to the solid suspension and left for overnight conditioning to reach adsorption equilibrium. The suspensions were then centrifuged and the supernatants pipetted out for determination of polymer concentration by a Total Organic Carbon Analyzer. The adsorption density of the polymer on the solid was calculated from the data for initial and residual polymer concentrations.

#### 2.2.4. Colorimetric method

A colorimetric method described by Dubois et al. [20] was used in the experiments. Since phenol in the presence of sulfuric acid can be used for quantitative colorimetric microdetermination of polysaccharides, in this study, 0.05 ml 80% phenol and 5 ml 98% sulfuric acid were added to 2 ml of polymer supernatant obtained after centrifugation, and after 4 h of color development under warm conditions, absorbance was measured at a wavelength of 487.5 nm using SHIMADZU UV-1201 UV–vis spectrophotometer. Adsorption density of polymer on talc was calculated from the difference in absorbance.

#### 2.2.5. FTIR study

The infrared spectra of talc, polysaccharides and polymer adsorbed talc were recorded using a Model FTS7000 series Fourier transform infrared spectrometer from Digilab operating in the range 4000–350 $cm^{-1}$. The KBr pellet technique was adopted for recording the spectra. Specifically speaking, the solid samples were obtained through following the procedure of adsorption measurement mentioned above (the solids were dried afterwards). Approximately 2 mg of the desired powder sample was thoroughly mixed with 200 mg of spectroscopic grade KBr and pressed into pellets for recording the spectra.

#### 2.2.6. AFM analysis

The atomic force microscopic (AFM) study was done with Nanoscope III (Digital instruments, Santa Barbara, CA). The measurements were performed underwater in tapping mode using a V-shaped $Si_3N_4$ cantilever covered with gold on the back for laser beam reflection. All images were collected in the height mode, which keep the force constant.

## 3. Results and discussion

### 3.1. Molecular modeling

Fig. 2 shows the computer simulated molecular space filling structures of guar gum and locust bean gum in both vacuum and aqueous environments. Each of them contains 5 repeat units. It is seen that polymer chains tend to be in a more stretched form

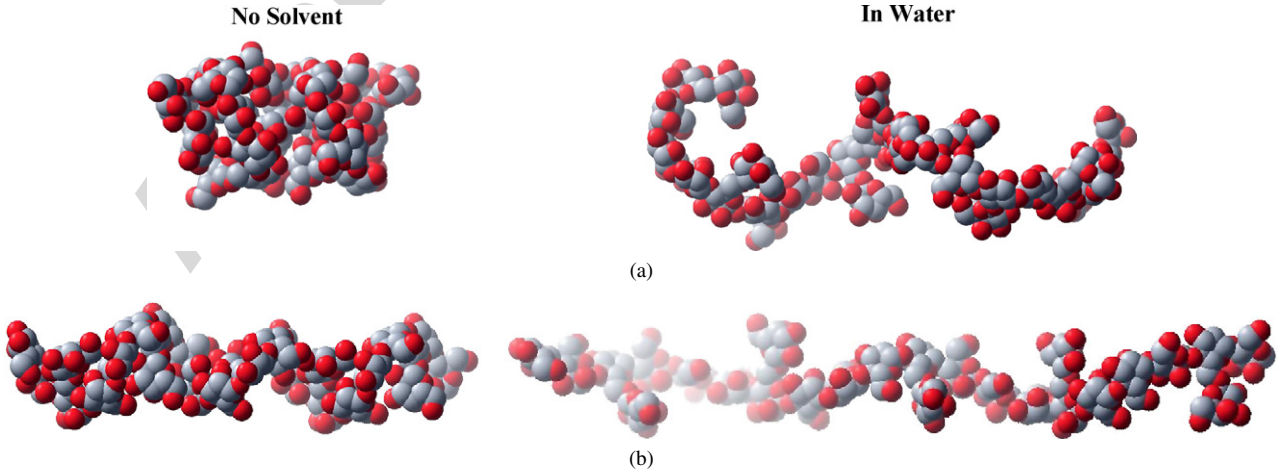


Fig. 2. Computer simulated molecular CPK (space filling) structure of (a) GG, (b) LBG with and without aqueous environment (each contains five repeat units).

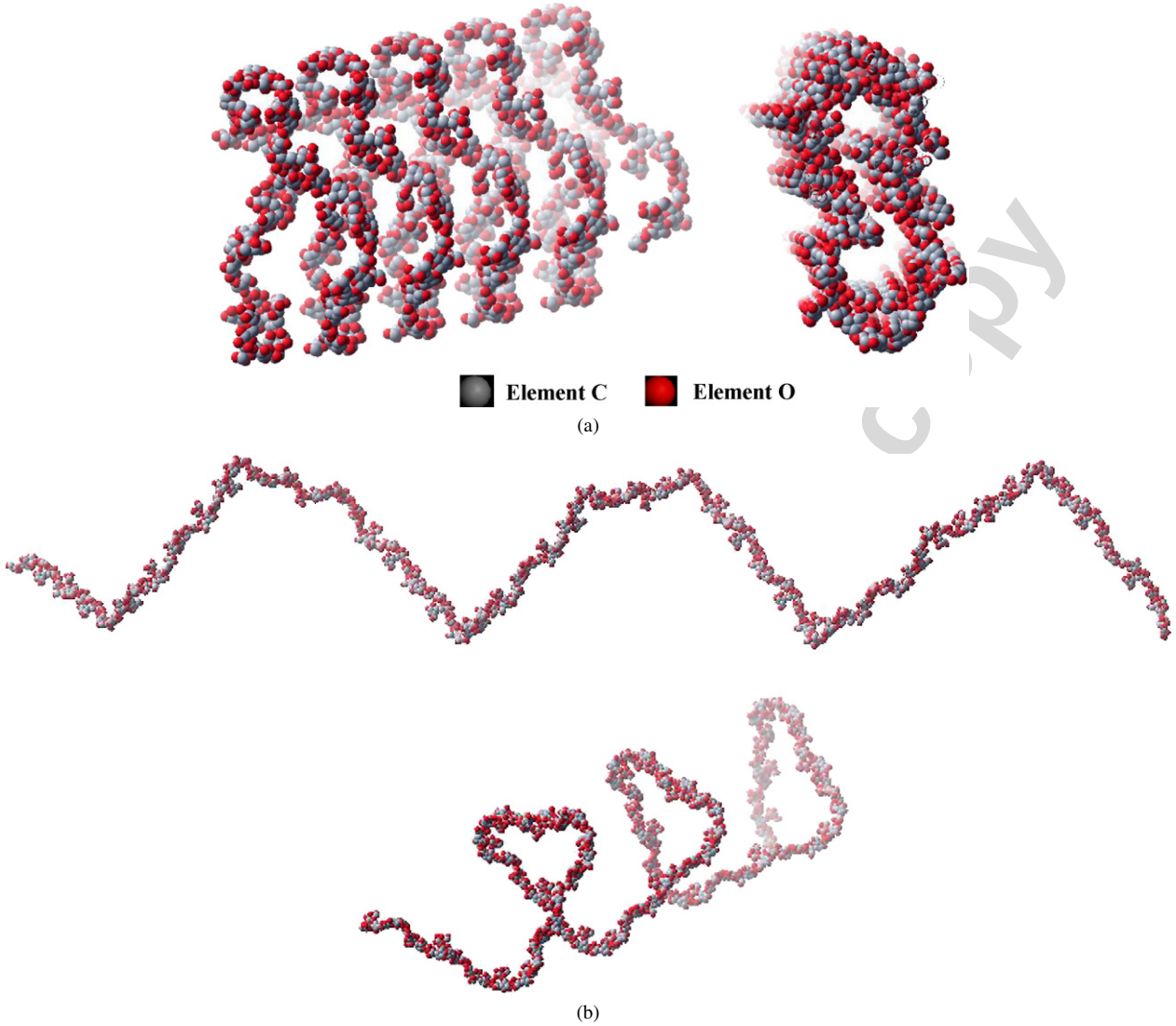


Fig. 3. Computer simulated latitudinal view and longitudinal view of molecular CPK (space filling) structure of (a) GG, (b) LBG in aqueous environment (each contains 50 repeat units).

in water than in vacuum. The helical structure shown in Fig. 3 is a piece of polymer chain containing 50 repeat units. GG forms a more complicated structure than LBG because of the increase in galactose units along the mannose chain. According to the simulation results, there is no change in the simulated structure when the number of repeat units on the chain is increased further to 100.

From computer simulation by Accelrys Material Studio (Fig. 4), the two galactomannose polymer molecules are seen to choose a relatively flat conformation on talc surface to let more of its OH groups in contact with the surface.

### 3.2. Electrokinetic studies

It is evident from the electrokinetic data shown in Fig. 5 that the surface of talc is negatively charged and the isoelectric point (iep) is located around pH 2.5. Above pH 2.5, the electronegative character increases with increase in pH up to pH 4 and thereafter remains almost constant. The adsorption of GG and LBG decreased the negative zeta potential of the talc (without any shift of iep) but did not reverse the charge, which indicates that the adsorption of these polymers only masks the surface charge on talc. Electrostatic interaction is not expected to be the dominant force in these systems.

### 3.3. Adsorption studies

Adsorption experiments have been conducted to study the effect of pH, ionic strength and urea on the adsorption of guar gum and locust bean gum on talc. The results are analyzed using Langmuir model to extract parameters relevant to the adsorption mechanism of polysaccharides on talc.

#### 3.3.1. Influence of pH

Fig. 6 shows the isotherms for the adsorption of LBG on talc at pH 3 and 9. It can be seen that the adsorption density does not vary measurably between pH 3 and 9. Similar results have also been reported in our previous paper for guar/talc system [21]. If

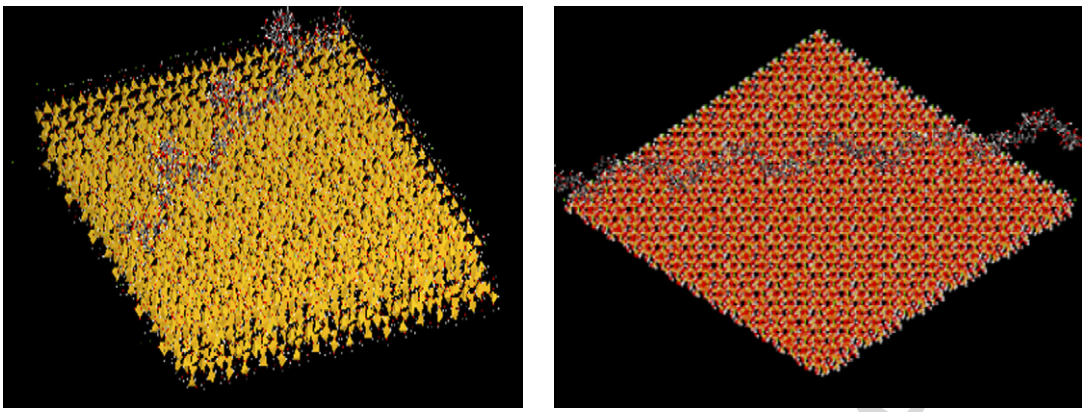

(b) (a)

Fig. 4. Computer simulated structure of (a) GG, (b) LBG molecule on talc surface.

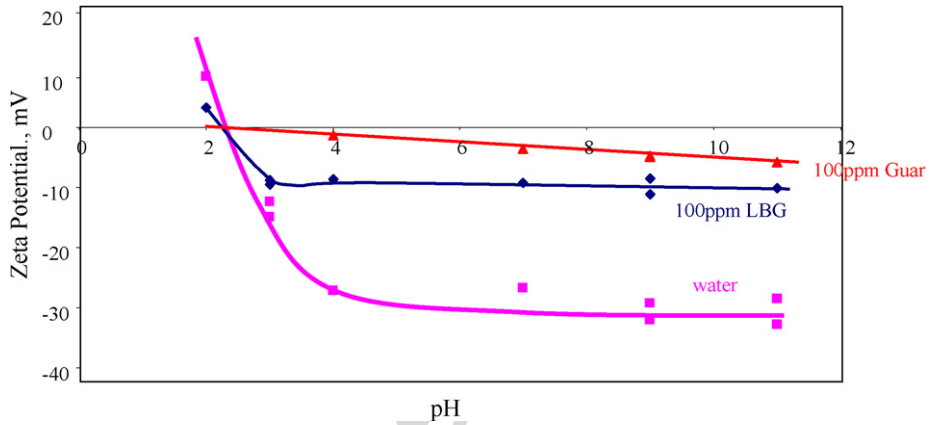


Fig. 5. Zeta potential of talc as a function of pH in the presence and absence of GG and LBG, IS = 0.001 M.

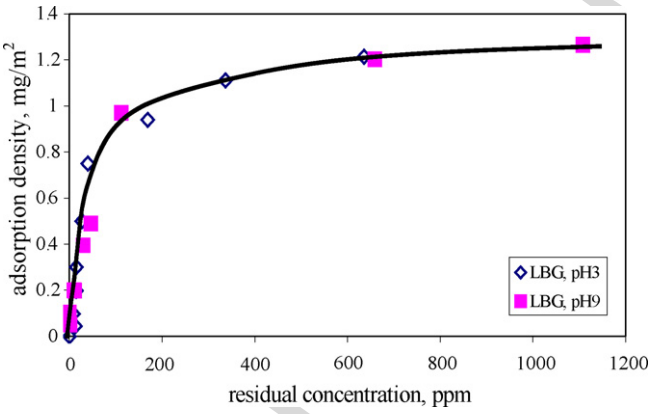


Fig. 6. Adsorption isotherm of LBG on talc at different pH.

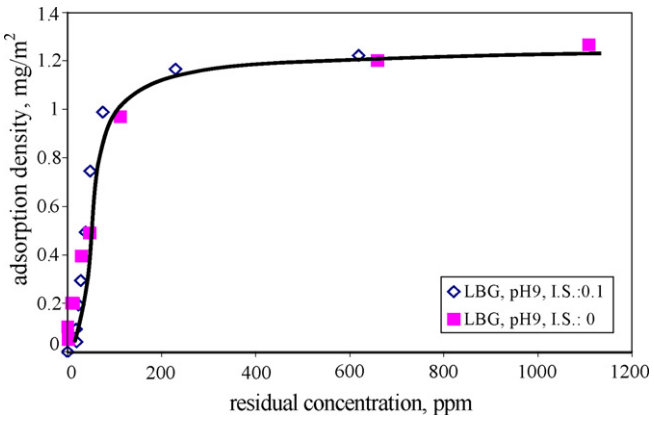


Fig. 7. Adsorption isotherm of LBG on talc at different ionic strengths.

electrostatic interaction plays an important role in the adsorption process, the adsorption density of polymer on talc should have been affected significantly since the surface charge of talc does change with change in pH from 3 to 9. Such is not the case here, and it can be concluded that electrostatic interaction is not the dominant force for the adsorption of LBG and GG on talc.

### 3.3.2. *Influence of ionic strength*

Adsorption isotherms of LBG on talc at different ionic strengths are shown in Fig. 7. The effect of ionic strength on guar adsorption on talc can also be found in our previous work [21]. If hydrophobic force makes a significant contribution to adsorption of a polymer on a mineral, the adsorption density would increase with the addition of salt due to "salting-out" effect [22]. For LBG, there is no significant change of the adsorption density as ionic strength is increased from 0 to 0.1. Thus it would appear that the hydrophobic force also is not the main driving force for the adsorption of LBG and GG on talc.

### 3.3.3. Adsorption on talc with and without urea

To examine the possible role of hydrogen bonding, adsorption tests were carried out in the presence of urea, a hydrogen bond breaker. Urea is a strong hydrogen bonding acceptor and it can affect the hydrogen bonding between the solid and the polymer in solution by preferential formation of hydrogen bonds between themselves and the polysaccharides or water. Adsorption isotherms for LBG on talc in the presence and absence of urea at pH 9 given in Fig. 8 show marked reduction in adsorption due to urea addition and similar results obtained previously for GG (see Fig. 9) [21]. A comparison of the results presented in this figure with the hydrogen bond breaker, urea, suggests that the hydrogen bonding plays a similar important role in the adsorption of GG and LBG on talc.

### 3.3.4. Modeling of polysaccharide adsorption on solid surface

To obtain a better understanding of the adsorption mechanism of galactomannose on solids, a number of parameters are extracted from the adsorption isotherms as shown in Table 1. standard free energy of adsorption $\Delta G^0_{\text{ads}}$, maximum amount of polymer adsorbed per mass of solid $(x/m)_{\max}$ and effective substrate area occupied per polymer chain $\sigma^0$ at the talc/solution interface.

The adsorption isotherms for GG and LBG onto solids measured in this study exhibited pseudo-Langmuirian behavior. According to Langmuir adsorption model applied to the polymer systems [23], surface coverage

$$\theta = KC/(1+KC) = (x/m)/(x/m)_{\max}. \tag{1}$$

Equation (1) can be expressed as

$$m/x = 1/\left[K(x/m)_{\max}C_{\text{eq}}\right] + 1/(x/m)_{\max}, \tag{2}$$

where $C_{\text{eq}}$ is the equilibrium solution concentration of polymer, $x$ as the amount of polymer adsorbed, $m$ as the mass of solid substrate, $K$ as the Langmuir adsorption equilibrium constant and $(x/m)_{\max}$ as the maximum amount of polymer adsorbed per mass of solid. A plot of $m/x$ against $1/C_{\text{eq}}$ should yield a linear relationship. The values of $K$ and $(x/m)_{\max}$ can be determined from the intercept and slope of such a plot as shown in Figs. 10 and 11.

The Langmuir adsorption equilibrium constant, $K$, can be considered to represent the affinity of a polymer for a particular surface. It can be related to the standard free energy of adsorp-

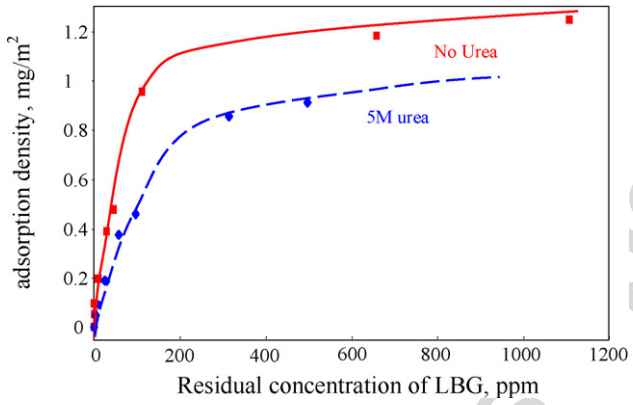


Fig. 8. Adsorption isotherms of LBG on talc with and without urea ($I = 0$, pH 9).

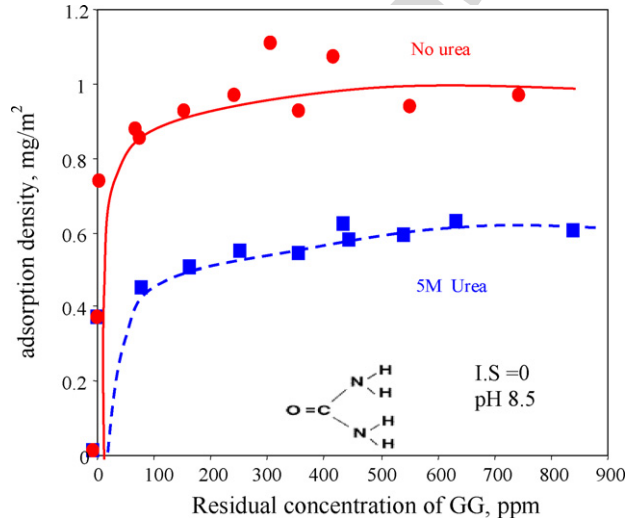


Fig. 9. Adsorption isotherms of GG on talc with and without urea ($I = 0$).

Table 1
The calculated values of $(x/m)_{\max}$, $\Delta G^0_{\text{ads}}$ and $\sigma^0$ for the adsorption of GG and LBG on talc at $T = 25\,^\circ\text{C}$

| Polymer | $(x/m)_{\max}$ (mg/m$^2$) | $\Delta G^0_{\text{ads}}$ (kJ/mol) | $\sigma^0$ (nm$^2$) |
|---|---|---|---|
| Guar (142C) | 0.98 | −21.3878 | 2457.39 |
| LBG | 1.18 | −24.4461 | 1411.657 |

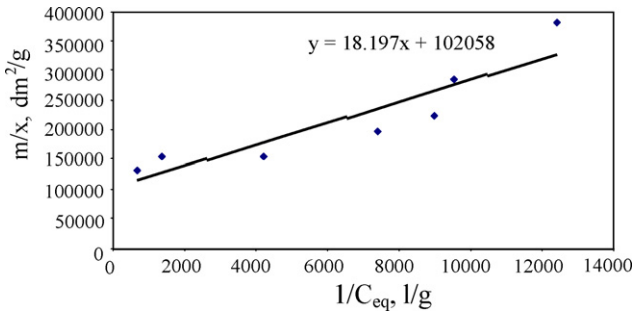


Fig. 10. Langmuir plot for adsorption of GG (142C) on talc at pH 9, $T = 25\,^\circ\text{C}$.

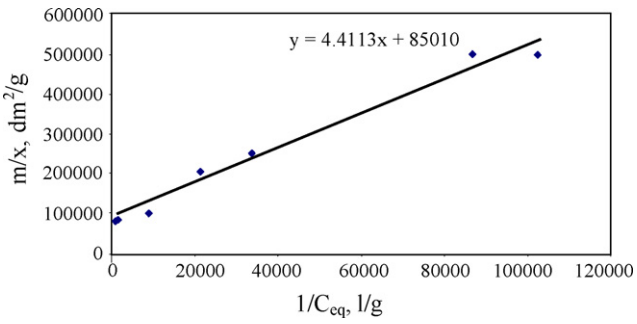


Fig. 11. Langmuir plot for adsorption of LBG on talc at pH 9, $T = 25\,^\circ\text{C}$.

tion, $\Delta G^0_{ads}$, from the expression given in Eq. (3):

$$\Delta G^0_{ads} = -RT \ln K, \tag{3}$$

where $R$ is the general gas constant ($R = 8.314$ J/(mol K)) and $T$ as the absolute temperature.

From the maximum adsorption density, the effective area occupied on the substrate surface per polymer chain, $\sigma^0$, can be calculated using the following equation:

$$\sigma = \theta \frac{A}{n_2^s N_A}, \tag{4}$$

where $N_A$ is Avogadro's number. $\theta$ is the fraction of the surface covered by polymer, $A$ as the substrate surface area, $n_2^s$ as the number of moles of polymer adsorbed.

The number of moles of polymer adsorbed per unit area of solid, $n_2^s/A$, is given by equation

$$\frac{n_2^s}{A} = \frac{(x/m)_{max}}{M_w}, \tag{5}$$

where $M_w$ is the molecular weight of the polymer. Hence, the effective substrate area occupied per polymer molecule, $\sigma^0$, can be calculated using equation

$$\sigma^0 = \theta \frac{M_w}{(x/m)_{max} N_A}. \tag{6}$$

From Table 1, it can be seen that $\Delta G^0_{ads}$ for the two galactomannose indicate that adsorption of this polymer on talc is highly favourable, i.e. $\Delta G^0_{ads} < 0$. As is well known, the free energy of hydrogen bond formation is about −25 kJ/mol, which is very close to the $\Delta G^0_{ads}$ of the polymers, −22 kJ/mol. Moreover, if hydrophobic interaction is the major force for adsorption, then a value of −50 kJ/mol can be expected for $\Delta G^0_{ads}$ [24], which is much greater than the calculated value. Therefore, the theoretical results further confirm the major role of hydrogen bonding rather than hydrophobic force in polysaccharide adsorption.

For a particular polymer, the value of $\sigma^0$ will be determined by the conformation that the polymer adopts upon adsorption. Clearly, $\sigma^0$ will be much greater if the polymer is adsorbed mainly in "trains" (a conformation in which the majority of the polymer is in contact with the surface) than if it adsorbs in the form of a high degree of "loops" and "tails" (one in which a lower proportion of the polymer segments are in contact with the surface). As shown in Table 1, the $\sigma^0$ of GG and LBG are very high, which suggests that most segments of these polymers are adsorbed in a flat conformation on the talc surface.

### 3.4. FTIR spectroscopy

#### 3.4.1. Guar–talc system

Fig. 12 shows the spectra of talc, guar gum and guar gum adsorbed talc. The FTIR spectrum of talc is shown in Fig. 12a. According to the characteristic IR frequencies of talc reported by other researchers [25], the band at around 1039 cm$^{-1}$ can be assigned to the out-of-plane symmetric Si–O–Si mode. The Si–O bending vibration for talc has been observed at 432 cm$^{-1}$ in the spectrum. The other bands in the spectrum around 654, 604, 550, 481 and 450 cm$^{-1}$ are probably associated with various Mg–OH modes. The band at around 384 cm$^{-1}$ appears to involve mixed vibrations of the Si–O network, the octahedral cations and the hydroxy groups. The band at 374 cm$^{-1}$ is associated with a symmetric Mg–OH vibration. Talc also shows a single Mg–OH stretching band around 3677 cm$^{-1}$ due to the centrosymmetric relationship between the hydroxy groups on both sides of the octahedral layers.

For pure guar gum (Fig. 14), the band at 3430 cm$^{-1}$ represents O–H stretching vibration. The band at 2924 cm$^{-1}$ is due to C–H stretching of the –$CH_2$ groups. The bands due to ring stretching of galactose and mannose appear at 1641 and 1657 cm$^{-1}$. In addition, the bands in the region 1350–1450 cm$^{-1}$ are due to symmetrical deformations of $CH_2$ and COH groups. The bands due to primary alcoholic –$CH_2$OH stretching mode and $CH_2$ twisting vibrations appear at 1078 and 1021 cm$^{-1}$, respectively. The bands around 890 cm$^{-1}$ can be attributed to the C1–H deformation. The weak bands around 770 cm$^{-1}$ are due to ring stretching and ring deformation of $\alpha$-D-(1-4) and $\alpha$-D-(1-6) linkages.

The FTIR spectrum of talc after interaction with guar gum is depicted in Fig. 12. Weissenborn et al. [26] pointed out that the major difference between the non-adsorbed and adsorbed polysaccharide spectra occurred at round 1000 cm$^{-1}$ and this was observed in our study. It is clear that there are two strong bands and three weak bands on the spectrum in the re-

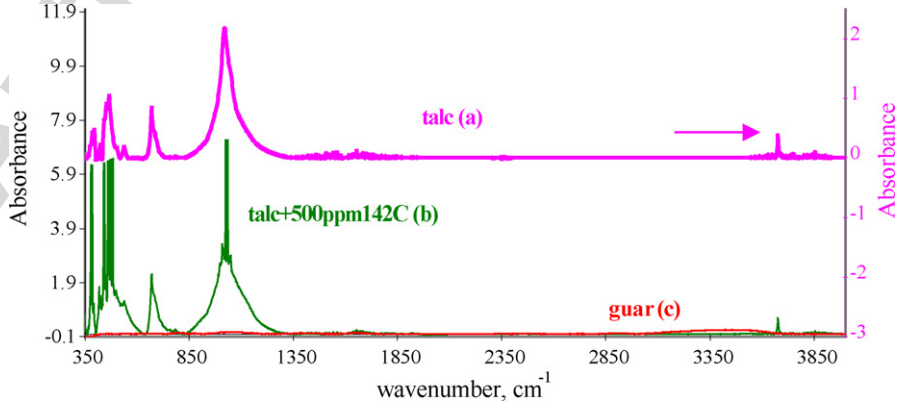


Fig. 12. FTIR spectra of (a) talc, (b) guar adsorbed talc and (c) guar gum.

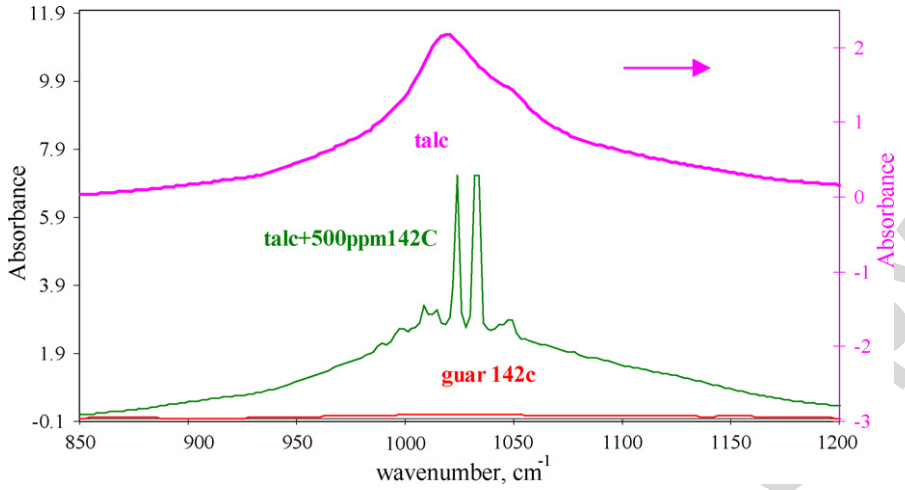


Fig. 13. FTIR spectra of talc, guar gum and guar adsorbed talc (850–1200 $cm^{-1}$).

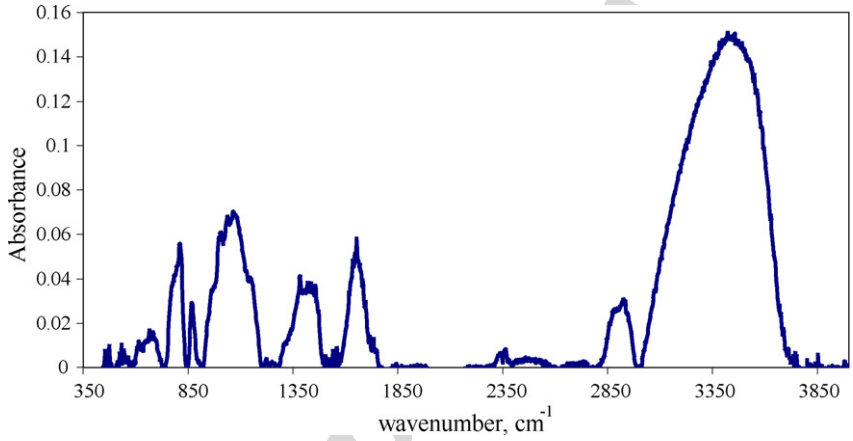


Fig. 14. FTIR spectrum of guar gum (in solid powder form, 350–4000 $cm^{-1}$).

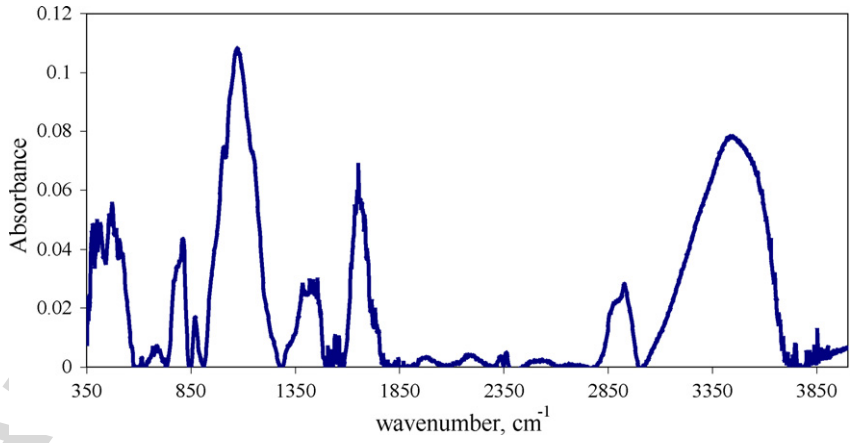


Fig. 15. FTIR spectrum of locust bean gum (in solid powder form, 350–4000 $cm^{-1}$).

gion 1000–1050 $cm^{-1}$ (Fig. 13), which is due to the hydrogen bond formation between the primary alcoholic $–CH_2OH$ and Si–O–Si after adsorption.

### 3.4.2. *LBG–talc system*

For pure locust bean gum (Fig. 15), the band at 3430 $cm^{-1}$ represents O–H stretching vibration. The band at 2924 $cm^{-1}$ is due to C–H stretching of the $–CH_2$ groups. The bands due to ring stretching of galactose and mannose appear at 1641 and 1657 $cm^{-1}$. In addition, the bands in the region of 1350–1450 $cm^{-1}$ are due to symmetrical deformations of $CH_2$ and COH groups. The bands due to primary alcoholic $–CH_2OH$ stretching mode and $CH_2$ twisting vibrations appear at 1078 and 1021 $cm^{-1}$ respectively. The weaker bands around 770 $cm^{-1}$

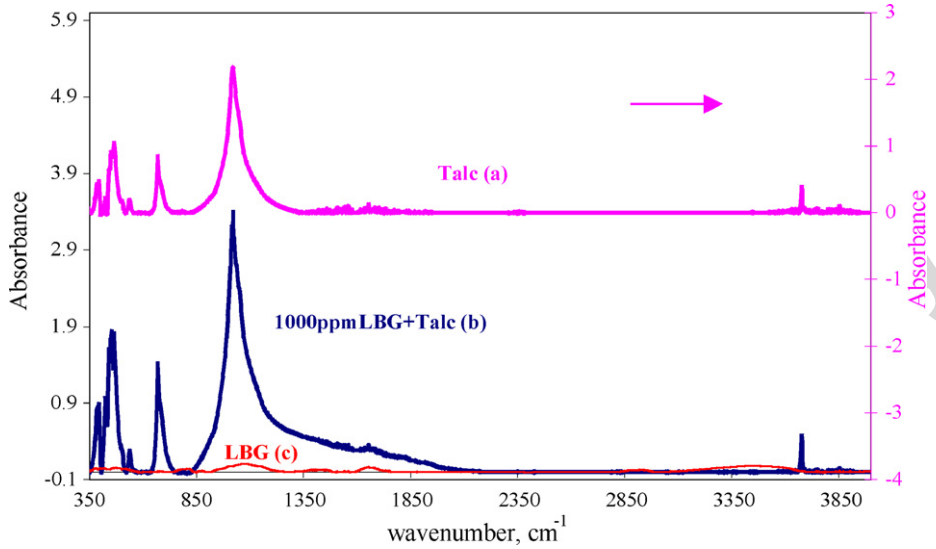


Fig. 16. FTIR spectra of (a) talc, (b) LBG adsorbed talc and (c) LBG.

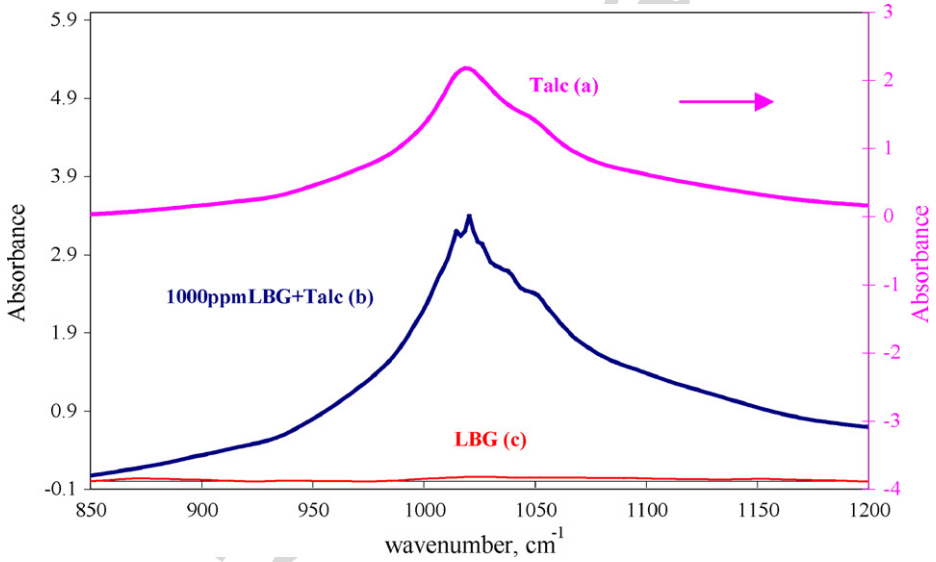


Fig. 17. FTIR spectra of talc, LBG and LBG adsorbed talc (850–1200 $cm^{-1}$).

are due to ring stretching and ring deformation of $\alpha$-D-(1-4) and $\alpha$-D-(1-6) linkages.

The spectrum of the LBG adsorbed talc is given in Fig. 16b. The most intense bands for the adsorbed LBG occurred in the region of 1000–1050 $cm^{-1}$ (Fig. 17), which is due to the hydrogen bond formation between the primary alcoholic $-CH_2OH$ and Si–O–Si after adsorption.

### 3.5. AFM studies

#### 3.5.1. Influence of polysaccharide concentration

From AFM study [27–30] of adsorbed guar gum at different concentration, it was found that guar gum first adsorb in the form of small clusters of about 1 nm thickness (Fig. 18a). Below maximum adsorption, the size of clusters increased with the increase in concentration (Fig. 18b), and further covered the surface fully with higher thickness (Fig. 18c), which suggest that GG forms a more densely packed compact conformation on the solid surface upon complete adsorption.

#### 3.5.2. Influence of mannose/galactose ratio of polysaccharide

AFM was employed to further study the adsorbed topography of LBG and GG on solid. From Fig. 19, the surface coverage of these two different galactomannose on mica does not vary much. But LBG adsorbs in the form of isolated clusters with higher vertical distance. On the contrary, GG forms larger islands with lower thickness at the same concentration. From our computer simulation, it is apparent that LBG has more flexible structure than GG. In addition, since the galactose/mannose ratio of LBG is lower than GG, the number of OH group on LBG that can form hydrogen bond with the solid surface is much less than that of GG, which explains why GG has a relatively flat conformation with lower thickness than LBG.

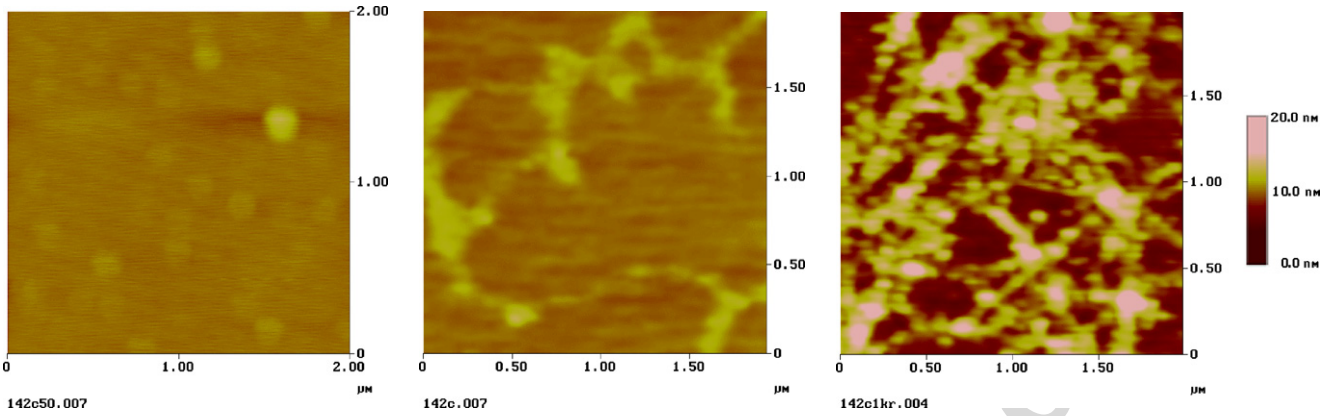


(a) (b) (c)

Fig. 18. AFM images of guar gum adsorbed on mica at concentration of (a) 50, (b) 200, and (c) 1000 ppm.

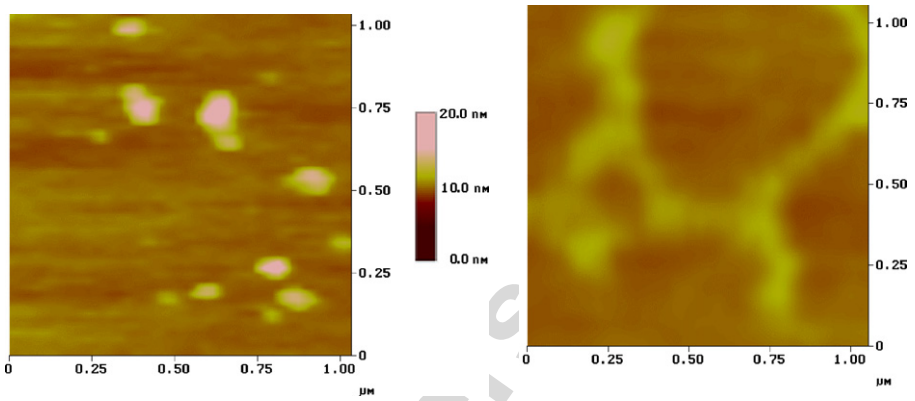


(a) (b)

Fig. 19. AFM images of gum with different M/G adsorbed on mica at (a) LBG, (b) GG (C: 200 ppm).

## 4. Conclusions

(1) From molecular modeling, a helical structure is observed in solution. The polymer was found to adsorb flat on solid surface to let more of its OH groups in contact with the surface.

(2) Electrokinetic studies of adsorption of LBG and GG on talc in the pH range of 2–11 showed that galactomannose decreased the negative zeta potential of talc without any shift of the iep. In addition, adsorption studies also showed that the adsorption of these polymers on talc is not affected by changes in pH and ionic strength. These results suggest the minor role of the electrostatic force in the adsorption process.

(3) Urea, a hydrogen bond breaker, reduces the adsorption of LBG on talc similar to GG/talc system. This result supports a mechanism involving hydrogen bonding rather than a hydrophobic one.

(4) Langmuir modeling of adsorption isotherm further supports the hydrogen bonding as the dominant force for polysaccharide adsorption since the adsorption free energy of these polymers is close to that of the hydrogen bond formation. Polysaccharides were also found to adsorb in a very flat conformation according to the calculated effective area occupied on the substrate surface per polymer chain and AFM analysis.

(5) FTIR study of polysaccharide-solid systems provides data on spectral changes that could be associated with hydrogen bonding between polysaccharides and solid surfaces. The changes in the infrared bands in the region 1000–1080 $cm^{-1}$, associated with the C–O stretch coupled to the C–C stretch and O–H deformation, were significant and therefore suggest strong hydrogen bonding of polysaccharides to the solid surfaces.

All the above results suggest the main driving force for GG and LBG adsorption on talc to be hydrogen bonding rather than electrostatic or hydrophobic force. No effect of galactose to mannose ratio is observed for polysaccharide adsorption behavior. In addition, conformational studies suggest a helical structure of GG and LBG in solution while they are found to adsorb flat on the solid surface.

## Acknowledgments

The authors acknowledge the support of the National Science Foundation (Grant #CTS-00-89530, EEC-03-2861) and Cytec, Unilever, Uniquema, FIPR, DOE, ELKAY, Dispersion Technologies.

## References


[1] W.T. Winter, Y.Y. Chien, H. Bouckris, in: G.O. Phillips, D.J. Wedlock, P.A. Williams (Eds.), Gums and Stabilisers for the Food Industry, vol. 2, Pergamon, Oxford, 1984, pp. 535–539.
[2] J.M.W. Mackenzie, EGMJ (October 1980) 80–87.
[3] D. Reichman, N. Garti, in: E. Dickinson (Ed.), Food Polymers, Gels and Colloids, Royal Society of Chemistry, Cambridge, 1990, pp. 549–557.
[4] D. Reichman, N. Garti, in: G.O. Phillips, D.J. Wedlock, P.A. Williams (Eds.), Gums and Stabilisers for the Food Industry, vol. 5, IRL Press, Oxford, 1990, pp. 441–446.
[5] D. Reichman, N. Garti, Food Struct. 12 (1993) 411–426.
[6] D. Reichman, Ph.D. thesis, The Hebrew University of Jerusalem, Israel (1992).
[7] N. Garti, D. Reichman, Food Hydrocolloids 8 (1994) 155–173.
[8] C. Viebke, L. Piculell, Carbohydr. Polym. 29 (1) (1996) 1–5.
[9] V.R. Sinha, R. Kumria, Int. J. Pharm. 224 (2001) 19–38.
[10] M. Mackenzie, in: D. Malhotra, W.F. Riggs (Eds.), Chemical Reagents in the Mineral Processing Industry, Society of Mining Engineers, Colorado, USA, 1986, pp. 139–145.
[11] R.J. Pugh, Int. J. Miner. Process. 25 (1989) 101–130.
[12] T.W. Healy, J. Macromol. Sci. Chem. A 8 (1974) 603–619.
[13] R.K. Rath, S. Subramanian, Miner. Eng. 10 (1997) 1405–1420.
[14] R.K. Rath, S. Subramanian, J.S. Laskowski, Langmuir 13 (1997) 6260–6266.
[15] E. Steenberg, Ph.D. thesis, Faculty of Science, University of Potchefstroom, Johannesburg, South Africa (1982).
[16] E. Steenberg, P.J. Harris, S. Afr. J. Chem. 37 (1984) 85–90.
[17] P. Jenkins, J. Ralston, Colloids Surf. A 139 (1998) 27–40.
[18] R.K. Rath, S. Subramanian, J.S. Laskowski, in: J.S. Laskowski, G.W. Poling (Eds.), Processing of Hydrophobic Minerals and Fine Coal, Canadian Institute of Mining, Metallurgy and Petroleum, Montreal, Canada, 1995, p. 105.
[19] B.A. Jucker, H. Harms, S.J. Hug, A.J.B. Zehnder, Colloids Surf. B Biointerfaces 9 (1997) 331–343.
[20] M. Dubois, K.A. Gilles, J.K. Hamilton, P.A. Rebers, F. Smith, Anal. Chem. 28 (1956) 350–356.
[21] J. Wang, P. Somasundaran, D.R. Nagaraj, Miner. Eng. 18 (1) (2005) 77–81.
[22] G. Rexwinkel, B.B.M. Heesink, W.P.M. van Swaaij, J. Chem. Eng. Data 44 (1999) 1139–1145.
[23] D.J. Shaw, Introduction to Colloid and Surface Chemistry, Butterworth-Heinemann, Oxford, 1992.
[24] J.D. Miller, J.S. Laskowski, S.S. Chang, Colloids Surf. A 8 (1983) 137–151.
[25] J.T. Kloprogge, R.L. Frost, L. Rintoul, Phys. Chem. Chem. Phys. (1999) 2559–2564.
[26] P.K. Weissenborn, L.J. Warren, J.G. Dunn, Colloids Surf. A 99 (1995) 11–27.
[27] I. Capron, S. Alexandre, G. Müller, Polymer 39 (1998) 5725–5730.
[28] T.M. McIntire, R.M. Penner, D.A. Brant, Macromolecules 28 (1995) 6375–6377.
[29] A.P. Gunning, A.R. Kirby, M.J. Ridout, G.J. Brownsey, V.J. Morris, Macromolecules 29 (1996) 6791–6796.
[30] K.J. Wilkinson, E. Balnois, G.G. Leppard, J. Buffle, Colloids Surf. A 155 (1999) 287–310.